Table 9
The potential across the membrane consisting of a dialysis membrane, Nafion, the agar gel containing the saturated KCl, and Selemion

Notation	Left solution	Right solution	V_{exp} [mV]
dns1	0.01 M KCl	0.10 M KCl	−83
dns2	0.10 M KCl	0.10 M KCl	−78
dns3	0.10 M KCl	0.01 M KCl	−117
dns4	0.10 M KCl	0.10 M KCl	−78

Notes. Left solution ≡ the type of solution and its concentration in the left compartment. Right solution ≡ the type of solution and its concentration in the right compartment. V_{exp} ≡ the experimentally measured potential across the membrane consisting of a dialysis membrane, Nafion, the agar gel containing saturated KCl, and Selemion. dns4 is the same as dns2.

V_{exp}(dns2) given in Table 9 would be expected, if we waited for a long while before performing the potential measurement.

One may think that there exists a slight selective permeability for the left side membrane, and it might cause the potential change from $V_{exp}(\text{dns1}) = -83$ mV to $V_{exp}(\text{dns2}) = -78$ mV. However, the experimental observation of dns2 showed a nonzero potential, despite the same concentration of KCl in both compartments, just like the experiment ns1 in Table 8. The membrane theory cannot explain this. The relationship between V_{exp}(dns1) and V_{exp}(dns2) is also regarded as supportive evidence to the adsorption theory as explained next. V_{exp} is given by

$$V_{exp} = [\text{the potential in the right compartment}] - [\text{the potential in the left compartment}]. \quad (12)$$

Assuming the adsorption theory is valid in this experiment, [the potential in the right compartment] is speculated to be maintained constant concerning dns1 and dns2. Therefore V_{exp} of dns1 and dns2 is a function of [the potential in the left compartment] as given by

$$V_{exp} = \text{const} - [\text{the potential in the left compartment}]. \quad (13)$$

According to the potential behavior of n41 and n43 in Table 4, whose behaviors are in line with the adsorption theory as explained in Section 3.3.1, their potential decreases with increased KCl concentration from +99 to +74 mV. Employing this relationship for Eq. (13), we can obtain the relationship

$$\begin{aligned} V_{exp}(\text{dns1}) &= \text{const} - [\text{the potential of low conc. KCl in the left compartment}] \\ &< \text{const} - [\text{the potential of high conc. KCl in the left compartment}] \\ &= V_{exp}(\text{dns2}). \end{aligned} \quad (14)$$

So $V_{exp}(\text{dns1}) < V_{exp}(\text{dns2})$ is expected, and it agrees with our observation, $V_{exp}(\text{dns1}) = -83$ mV $< V_{exp}(\text{dns2}) = -78$ mV. This argument also brings us the relationship $V_{exp}(\text{dns3}) < V_{exp}(\text{dns4})$, and it agrees with the experimental results in Table 9. This evidence also strongly supports the validity of the adsorption theory.

4. Summary and conclusions

The potential of two ionic solutions across a membrane is determined by the sum of the potentials at individual interfaces between the ionic solution and the membrane, not the selective permeability of the membrane. The potential generation has nothing to do with the membrane permeability, but that there is an exposure of its adsorption sites to the ionic solution actually dominates the nonzero potential occurrence. These observations all agree with the adsorption theory but conflict with the membrane theory. We should reinterpret the results believed to be in line with the membrane theory now.

Acknowledgments

We express our gratitude to Nihon Polymer (Aichi, Japan) for their service to us many times to get Nafion sheets and also to Asahi Glass Co., Ltd. (Tokyo, Japan) for providing us Selemion sheets. This work was conducted under financial support by Health and Labor Science Research Grants of Research on Advanced Medical Technology (No. H14-nano-021) from the Ministry of Health Labor and Welfare, The Mikiya Science and Technology Foundation, and the Ogawa Foundation, all in Japan.

References

[1] G. Colacicco, Nature 207 (1965) 936.
[2] G.N. Ling, In Search of the Physical Basis of Life, Plenum, New York, 1984.
[3] K.L. Cheng, in: J.T. Stock, M.V. Orno (Eds.), ACS Symposium Series, vol. 390, 1989, p. 286.
[4] G.N. Ling, A Revolution in the Physiology of the Living Cell, Krieger, 1992.
[5] G.N. Ling, Physiol. Chem. Phys. Med. NMR 26 (1994) 121.
[6] B. Alberts, D. Bray, A. Johnson, J. Lewis, M. Raff, K. Roberts, P. Walter, Essential Cell Biology—An Introduction to the Molecular Biology of the Cell, Garland, New York, 1998 [Japanese edition, Nankodo, Tokyo, 1999].
[7] G.H. Pollack, Gels and the Engines of Life: A New, Unifying Approach to Cell Function, Ebner & Sons, Seattle, 2001.
[8] G.N. Ling, Life at the Cell and Below-Cell Level: The Hidden History of a Fundamental Revolution in Biology, Pacific Press, New York, 2001.
[9] P.W. Atkins, Physical Chemistry, second ed., Oxford Univ. Press, Northants, 1982.
[10] G. Ehrensvärd, L.G. Sillén, Nature 141 (1938) 788.
[11] K.L. Cheng, S.N. Kar Chaudhari, Microchim. Acta 1 (1981) 185.
[12] K.L. Cheng, Microchem. J. 72 (2002) 269.

Available online at www.sciencedirect.com
SCIENCE DIRECT
Journal of Colloid and Interface Science 275 (2004) 107–112
JOURNAL OF Colloid and Interface Science
www.elsevier.com/locate/jcis

An interpretation of amphoteric gel hardness variation through potential and hardness measurement

Hirohisa Tamagawa,[a,*] Fumio Nogata,[a] and Kazuyuki Yagasaki [b]

[a] *Department of Human and Information Systems, Faculty of Engineering, Gifu University, 1-1 Yanagido, Gifu 501-1193, Japan*
[b] *Department of Mechanical System Engineering, Faculty of Engineering, Gifu University, 1-1 Yanagido, Gifu 501-1193, Japan*

Received 23 September 2003; accepted 20 January 2004
Available online 5 March 2004

Abstract

The hardness variation of amphoteric gel according to the surrounding solution conditions is quite unique. It hardens and softens reversibly regardless of its molecular network density. But this has been understood merely qualitatively. For the purpose of elucidation of the details of its behavior, we performed quantitative potential and hardness measurements on it. We observed the constant potential of amphoteric gels, ~ -60 mV, regardless of their swelling ratio and hardness. Such observations can be interpreted as the maintenance of the constant charge density of $-COO^-$ for any amphoteric gel, and they are further interpreted as intermolecular salt-linkage formation/disruption dominating the hardness of amphoteric gels.

Keywords: Neutral gel; Anionic gel; Cationic gel; Amphoteric gel; Swelling ratio; Potential; Hardness; Salt linkage; Molecular network density; Cross-linking

1. Introduction

Polymer gels have quite unique properties. Their phase transition has attracted especially strong attention from a number of researchers [1,2]. Although numerous efforts have been made to elucidate amphoteric gels' nature, still it has not been well understood, and the realization of gel applications is far beyond our reach. The recent investigation of gels performed by H.T. and F.N. (two of the authors of this paper) and collaborators suggested quite intriguing facets of their hardness behavior [3,4]. We further investigated their nature and report some findings on it in this paper.

The commonly known anionic and cationic gels containing –COOH and $-NH_2$, respectively, exhibit hardness variation according to the solution conditions surrounding them [3,4]. This is explained in terms of molecular network density. Both anionic and cationic gels soften in the swollen state, that is, the low-molecular-network-density state, while they harden in the contracted state, that is, the high-molecular-network-density state. This is an intuitively acceptable explanation. Hardness of amphoteric gels containing two functional atomic groups, –COOH and $-NH_2$, varies significantly, too, according to the solution conditions surrounding them. Yet, their hardness variation cannot be explained in terms of their molecular network density, unlike that of anionic or the cationic gels. It has been suggested that amphoteric gel hardness is sometimes high even in the largely swollen state, that is, the low-molecular-network-density state. Namely, the molecular network density of amphoteric gels is not a predominant factor in their hardness. Indirect evidence was found supporting the conclusion that the cross-linking dominates the degree of amphoteric gel hardness and the amount of cross-linking reversibly varies with the environmental conditions [3,4]. As intuitively understood, the increase of gel volume results in the decrease of molecular network density, leading to the decrease of cross-linking density. But as we reported before, this phenomenon does not appear to be true for amphoteric gels, namely, the further formation of cross-linking called salt linkage appears to be promoted in amphoteric gels, even when their volume increases, consequently the cross-linking density of amphoteric gel becomes higher even in its larger volume state [3,4]. We have strongly speculated that the cross-liking density dominates the hardness of the amphoteric gel; that is, the increase of cross-linking density causes

* Corresponding author.
E-mail address: tmgwhrhs@cc.gifu-u.ac.jp (H. Tamagawa).

0021-9797/$ – see front matter
doi:10.1016/j.jcis.2004.01.039

the hardening of the amphoteric gel matrix, while the decrease of cross-linking density causes softening.

Amphoteric gels we have investigated contain both negatively and positively charged atomic groups, $-COO^-$ and $-NH_3^+$. They form a salt linkage, $-COO^-\cdots{}^+H_3N-$. So the hardness variation of amphoteric gels is primarily an electrostatic effect. Therefore the potential behavior within the gel must reflect the hardness behavior of amphoteric gels.

In this study, we performed potential measurement within neutral, anionic, cationic, and amphoteric gels along with measurement of their swelling ratios. We also performed quantitative measurement of their hardness, since our previous investigation went no further than qualitative measurement. Then we discussed the gel-hardening phenomenon through examination of the correlation between the potential and the hardness of gels.

2. Materials and methods

Basically four types of acrylamide-based gels—neutral, anionic, cationic, and amphoteric gels—were prepared, all plate-shaped. Further, as to anionic and amphoteric gels, five different types of anionic gels and four different types of amphoteric gels were prepared. The chemicals employed to prepare these gels are summarized in Table 1 along with their notations. Acrylamide and *N*,*N*-methylenebisacrylamide were purchased from Wako (Osaka, Japan). Acrylic acid, *N*,*N*,*N*′,*N*′-tetramethylethylenediamine, and ammonium persulfate were purchased from Kishida (Osaka, Japan), and allylaminehydrochloride was purchased from TCI (Tokyo, Japan).

The chemicals were dissolved in deionized water and poured into the plate-shaped mold. The solution was heated at 65 °C for 1 h. It has been known that the $-CONH_2$ atomic group of the acrylamide molecule can be hydrolyzed into a –COOH atomic group in highly concentrated NaOH solution [2–5]. Thus, four anionic gels—AN1, AN5, AN48, AN72—were prepared through the immersion of neutral gels, N0, in 1 M NaOH solution for 1, 5, 48, and 72 h, respectively. All of the amphoteric gels—AM1, AM5, AM48, AM72—were prepared through the immersion of cationic gels, CA0, in 1 M NaOH solution for 1, 5, 48, and 72 h, respectively. On the completion of synthesis, the gels were washed by repetitive immersion in deionized water and acetone alternately. Then they were all stored in deionized water until they reached the equilibrium state. The deionized water was replaced with new water at least once a day for 5 days, since ionic gels release ions and change the bathing deionized water condition, causing significant property changes of gels.

2.1. Potential measurement

We performed potential measurement on the gels. An Ag/AgCl electrode was stuck into the gel matrix, while counter Ag/AgCl electrode was placed in the bathing solution. The potential within the gel with respect to the potential of the bathing solution was measured using an HE-104 electrometer (HOKUTO DENKO Corp., Tokyo, Japan) in the manner depicted in Fig. 1. This experiment was performed under the atmosphere at room temperature.

2.2. Hardness measurement

Gel hardness is usually assessed by the use of a rheometer. However, access to rheometers is not easy, since they are not a commonly or widely used apparatus. On the other hand, Hertz contact theory is a quite simple method for hardness assessment on material in the static state [6]. We employed this theory to assess the gel hardness. This experiment was performed under the atmosphere at room temperature.

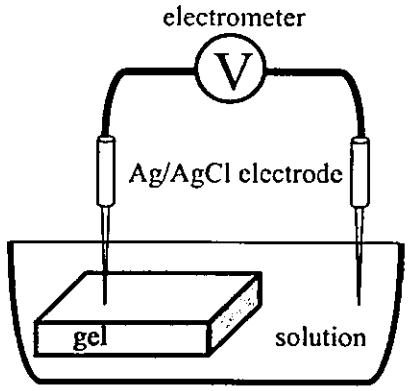

Fig. 1. Potential measurement setup. An Ag/AgCl electrode is stuck into a gel, and the Ag/AgCl counterelectrode is placed in the solution.

Table 1
The chemical weights employed for gel processing

Notation	AAm (g)	AAc (g)	AAHC (g)	MBA (g)	TEMED (g)	AP (g)	DW (g)
N0	11.56	0.00	0.00	0.154	0.10	0.08	100
AN0	8.52	2.87	0.00	0.154	0.10	0.08	100
CA0	8.52	0.00	3.72	0.154	0.10	0.08	100

Notes. N0, neutral gel; AN0–AN72, anionic gels; CA0, cationic gel; AM1–AM72, amphoteric gels; AN1–AN72 and AM1–AM72 were prepared through the hydrolysis of N0 and CA0, respectively, in 1 M NaOH solution for 1, 5, 48, and 72 h. AAm: acrylamide. AAc: acrylic acid. AAHC: allylaminehydrochloride. MBA: *N*,*N*-methylenebisacrylamide. TEMED: *N*,*N*-tetramethylethylenediamine. AP: ammonium persulfate. DW: deionized water.

Table 2
The potential, V, and swelling ratio, SR, of gels

	SR	V (mV)
N0	2.32	−10.88
AN0	11.72	−58.5
AN1	74.75	−56.2
AN5	112.85	−64.2
AN48	90.57	−59.9
AN72	103.18	−61.4
CA0	19.13	+26.5
AM1	36.5	−57.5
AM5	55.4	−57.2
AM48	96.9	−60.1
AM72	95.8	−59.4

Notes. Swelling ratio, SR, is defined by SR = [(thickness of water swollen gel)/(thickness of gel right after its synthesis)]^3.

3. Results and discussion

3.1. Gel potential

Table 2 shows the potential and swelling ratio of gels, where their swelling ratio, SR, is defined by SR = [(thickness of water swollen gel)/(thickness of gel right after its synthesis)]^3. Neutral, anionic, and cationic gel potentials are almost neutral, negative, and positive, respectively. This suggests that the sign of the potential within the gels is determined by the sign of the fixed charge contained in them. The anionic gel contains the fixed negative charge of $-COO^-$, causing a negative potential, while the cationic gel contains the fixed positive charge of $-NH_3^+$, causing a positive potential. The neutral gel, N0 contains no fixed charges and its potential, −10.88 mV, is the closest to 0 mV among all the gels.

What attracts our attention is that the potentials of AN0–AN72 are maintained constant at ∼ −60 mV, although their chemical compositions and the processing procedures are different and their swelling ratios are different, too. This suggests that the charge density in these gels is the almost same regardless of their swelling ratios. This can be easily explained by a commonly known concept of the chemical reaction. The reaction

$$-COOH \Leftrightarrow -COO^- + H^+ \quad (1)$$

occurs in the anionic gels.

Since the dissociation constant of this chemical reaction is constant as long as the environmental temperature is constant, the concentrations of –COOH, $-COO^-$, and H^+ contained in the five anionic gels, AN0–AN72, should be constant. Therefore the charge densities of $-COO^-$ atomic groups are the same, causing the same potential, although the swelling ratios are different due to the different amounts of –COOH created in AN0–AN72.

In order to fully confirm the potential maintenance of ∼ −60 mV for the anionic gels regardless of their swelling ratio, we performed the following experiment: Nakano et al. reported that the plate-shaped acrylamide gel can be brought into a curved shape in the equilibrium swollen state in deionized water as depicted in Fig. 2 by locally hydrolyzing the gel matrix [7]. This gel was originally a straight neutral gel; then only the top layer of it was hydrolyzed significantly in 0.1 M NaOH solution (see Fig. 2 again). The top layer came to have –COOH groups, which have a high affinity to water molecules. Therefore once this gel was immersed in the deionized water, it swelled with different degrees of swelling ratio along its thickness, causing the gel-shape to curve as in Fig. 2. Namely, the swelling ratio increases from the bottom layer toward the top layer. We applied this method to the anionic gel, AN0. Three different types of AN0 whose top layer was hydrolyzed in 0.1 M NaOH solution for 10, 20, and 30 min, respectively, were prepared, and they were designated as AN0-10, AN0-20, and AN0-30, respectively. Since the intact AN0 originally contained –COOH groups, all of AN0-10, AN0-20, and AN0-30 contain enough –COOH to generate a negative potential at least reaching ∼ −60 mV. They were immersed in the deionized water, and all of them deformed into the curved shape. After they reached equilibrium, the potential behavior within them along their thickness direction was probed by sticking Ag/AgCl electrodes into their gel matrix, where the Ag/AgCl counterelectrode was placed in the deionized water bathing them. We observed the virtually constant potentials for all of AN0-10, AN0-20, and AN0-30, regardless of the electrode tip depth from the gel top surface. Potential deviation was within only about 1 mV, even when the electrode tip depth was displaced by a few mm. Therefore undoubtedly the constant potential is realized through the maintenance of a constant charge density of $-COO^-$, resulting in a swelling ratio change. This strongly suggests that the potentials AN0–AN72 are maintained constant at ∼ −60 mV autonomously.

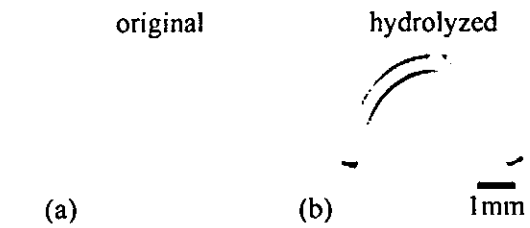

Fig. 2. Gel curving. The nonhydrolyzed straight acrylamide gel in photo (a) curves as shown in photo (b) through the hydrolysis of its upper part.

We have to add some comments on this measurement. From our investigation, the potentials within AN0-10, AN0-20, and AN0-30 virtually did not deviate. However, in the extreme vicinity of these gels' top and bottom surfaces within their matrices, the potentials decay by a few tens of mV. This could be explained by the concept put forward by Ling [8–11]. Ling suggested that injury to biological cells disturbs the activity of ions in the cell. This gives rise to a cell potential disturbance. Since the nature of the gel has been considered to be quite similar to that of a cell, this concept

of potential disturbance in the cell injury must be applicable as the cause of the gel potential decay. The surfaces of AN0-10, AN0-20, and AN0-30 are undoubtedly directly exposed to the external bathing solution, not protected by the rest of gel matrix. So their surfaces are continuously attacked by the bombardment of the surrounding water molecules. This must cause a potential disturbance of the gel at the surface, causing potential decay.

Regarding amphoteric gels, AM1–AM72, all of them exhibit negative potentials, although their starting materials are the same cationic gel, CA0, which exhibited the positive potential in Table 2. This suggests that –COOH created in amphoteric gels through their hydrolysis dominates the potential generation rather than $-NH_2$. In fact, their potentials are virtually constant, ~ -60 mV, which is the same as those of AN0–AN72 containing –COOH atomic groups, although their large swelling ratio difference goes to about 2.5-fold. To explain this phenomenon, we can speculate that the concentrations of –COOH, $-COO^-$, and H^+ in AM1–AM72 are constant, regardless of their swelling ratios, just like AN0–AN72, described in Section 3.1. Besides that, the swelling ratio behavior of amphoteric gel, for instance AM5, in the pH solutions is quite similar to that of anionic gel, AN0, as shown in Figs. 3a and 3c. Both AM5 and AN0 exhibit quite large swelling ratios in the high-pH solutions and quite small swelling ratios in the low-pH solutions. This suggests the occurrence of the reactions $-COOH \rightarrow -COO^+ + H^+$ in the high-pH solutions and $COOH \leftarrow COO^- + H^+$ in the low-pH solutions for both gels, since –COOH has a preventive effect on gel swelling due to the formation of hydrogen bonds and $-COO^-$ has a promotional effect on gel swelling due to the high affinity of its charge to the water molecules. Therefore –COOH rather than $-NH_2$ is the predominant atomic group for the potential behavior of amphoteric gels. In addition to this, the swelling ratio behavior of cationic gels containing $-NH_2$ atomic groups, CA0, is totally different from that of AM5, as shown in Fig. 3b. CA0 exhibits a large swelling in the low-pH solutions.

3.2. Gel hardness

The Young's moduli of gels, E_{gel}, was evaluated by employing the Hertz contact theory [6]. We placed several different sizes and weights of quite hard ceramic balls on the plate-shaped gels and measured the depth of the hollow, D_{gel}, created by these balls on the gel surfaces (see Fig. 4). The radius of the contact area between the gel and the ball, $R_{contact}$, is given by the simple calculation $R_{contact} = (2R_{ball}D_{gel} - D_{gel}^2)^{1/2}$, where R_{ball} is the radius of the ball placed on the gel surface (see Fig. 4). According to the Hertz contact theory, the relationship between the gel Young's modulus and the contact area radius is given by

$$R_{contact}^3 = (3/4)R_{ball}\left[\left(1-\nu_{ball}^2\right)/E_{ball} + \left(1-\nu_{gel}^2\right)/E_{gel}\right] \times (W_{ball}g), \quad (2a)$$

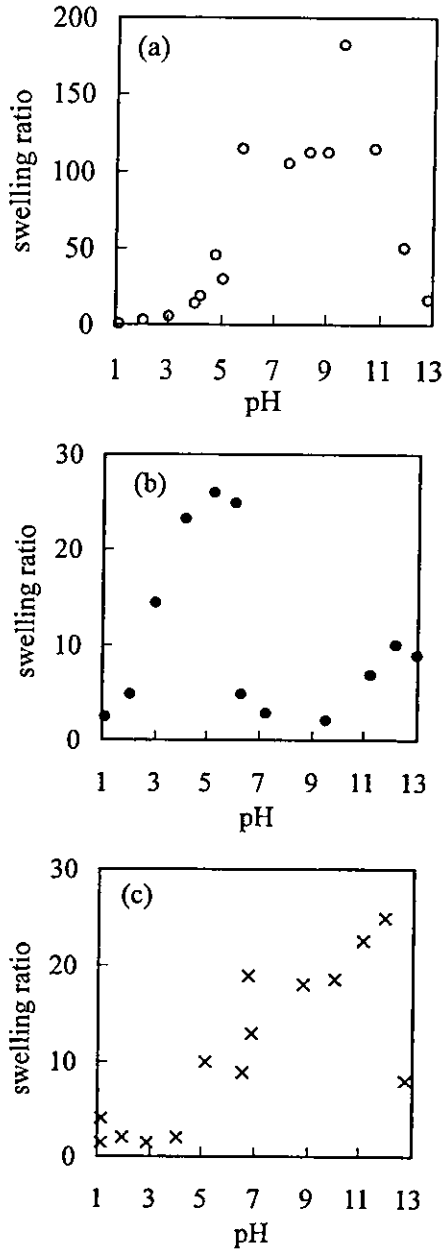

Fig. 3. pH dependence of gel swelling ratio: (a) AN0, (b) CA0, (c) AM5.

where E_{ball}, ν_{ball}, and W_{ball} are the Young's modulus, Poisson ratio, and weight of the ceramic ball, respectively, and ν_{gel} and g are the Poisson ratio of the gel and the gravitational acceleration, respectively. Under the assumptions $E_{ball} \gg E_{gel}$ and $\nu_{gel} = 1/2$, Eq. (2a) is simplified and rearranged into

$$R_{contact}^3 = (9/16)(R_{ball}W_{ball}g)/E_{gel}. \quad (2b)$$

From Eq. (2b), the Young's moduli of all gels were calculated. Table 3 shows the Young's moduli of gels. Young's moduli of AN1–AN72 are all less than that of N0. AN1–AN72 were prepared through the hydrolysis of N0; that is, their major structures are basically the same. However,

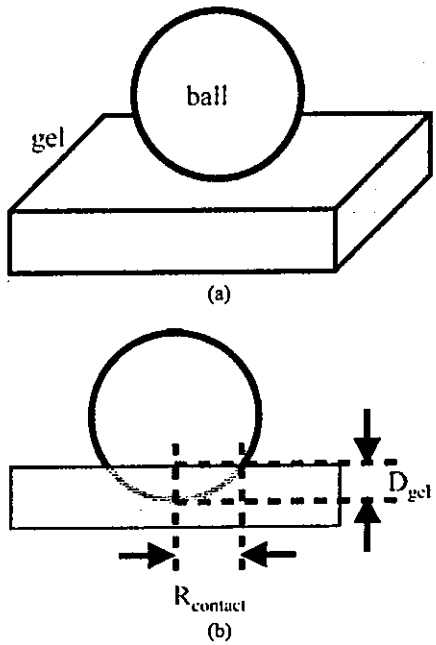

Fig. 4. Schematic illustration of hardness measurement on the gels: (a) overhead view; (b) side view.

Table 3
The Young's modulus, E_{gel}, of gels

	E_{gel} (MPa)
N0	0.012
AN0	0.006
AN1	0.011
AN5	0.008
AN48	0.011
AN72	0.008
CA0	0.005
AM1	0.011
AM5	0.010
AM48	0.007
AM72	0.008

the amounts of –COOH contained in them are strongly speculated to be different from one another because of their different duration of hydrolysis. Therefore the smaller Young's modulus of AN1–AN72 than N0 must be due to the larger swelling ratio of AN1–AN72 compared with N0. Their swelling ratios are about several tens of N0. Namely, the molecular network densities of AN1–AN72 are several tenths of N0, resulting in their lower Young's moduli. One may think that it is against his or her intuition that the Young's modulus of N0 is not significantly smaller than those of AN1–AN72, despite the observation of the extremely smaller swelling ratio of N0 than of AN1–AN72. The following is our answer to this question: Although we have not identified what causes this phenomenon exactly, we strongly suspect the formation of additional cross-linkings hydrogen bonds between –COOHs contained in AN1–AN72, and they could reinforce their matrices comparably to the hardness of N0. Although the duration times of hydrolysis of AN1–AN72 are different from one another, which creates the different amounts of –COOH contained in AN1–AN72, there was not such significant differences among their Young's moduli. It also can be explained through the creation of hydrogen bondings and the maintenance of the constant concentration of –COOH as described in Section 2.1. Namely, regardless of the swelling ratio, the density of cross-linking hydrogen bonds was maintained constant. Therefore as long as the hardness of AN1–AN72 is dominated primarily by the hydrogen bonds, their Young's moduli could be maintained almost constant regardless of their swelling ratio. This explanation is quite consistent with the discussion in Section 2.1.

AM1–AM72 were prepared through the hydrolysis of CA0; that is, their major structures are basically the same. However, the amounts of –COOH contained in them are strongly speculated to be different because of the different duration time of hydrolysis and their large variation of swelling ratio (see Table 2). Young's moduli of AM1 and AM5 are about twofold CA0's Young's modulus. However, the swelling ratios of AM1 and AM5 are both two- to threefold larger than that of CA0. Namely, the molecular network densities of AM1 and AM5 are both lower than that of CA0, yet still their Young's moduli are larger than that of CA0. As was reported before, this phenomenon was speculated to be caused by the formation of intramolecular salt linkages between –COOH and $-NH_2$, $-COO^-\cdots{}^+H_3N-$ [3,4]. Salt linkages serve as additional cross-linkings reinforcing the matrices of AM1 and AM5. The swelling ratios of AM48 and AM72 are much larger than that of CA0, yet still their Young's moduli are larger than CA0. This suggests that the gel matrix reinforcement by the salt linkages is quite effective. AM48 and AM72 have the larger swelling ratios and the smaller Young's moduli than AM1 and AM5. This must be due to the creation of larger amounts of –COOH in AM48 and AM72 than in AM1 and AM5 due to the longer hydrolysis duration of AM48 and AM72 than of AM1 and AM5. Namely, the larger amount of $-COO^-$ must exist through the dissociation of a larger amount of –COOH in AM48 and AM72; thus AM48 and AM72 swell until their fixed charge density of $-COO^-$ is the same as those of AM1 and AM5. In other words they swelled until the potential of ~ -60 mV was realized. This resulted in larger swelling ratios of AM48 and AM72 than of AM1 and AM5 and led to lower molecular network densities (or smaller Young's moduli) of AM48 and AM72 than of AM1 and AM5. Concerning this point, one question may be raised: that AM48 and AM72 have a higher opportunity to form salt linkages, compared with AM1 and AM5, because of the presence of more –COOH in them than in AM1 and AM5, so that the Young's moduli of AM48 and AM72 should be larger than those of AM1 and AM5. In spite of this plausible speculation, smaller Young's moduli of AM48 and AM72 than of AM1 and AM5 were observed. This could be explained by the lack of the counterpart of $-COO^-$, that is, $-NH_3^+$, to form salt linkages in

AM48 and AM72. All of AM1, AM5, AM48, and AM72 definitely have the same amount of $-NH_2$ in their bodies. In the swollen state, some $-NH_2$ is converted into $-NH_3^+$, which can serve as a counterpart of $-COO^-$ for the formation of a salt linkage. Although AM48 and AM72 contain larger numbers of $-COO^-$, the number of $-NH_3^+$ is limited. Therefore the increase in the number of $-COO^-$ cannot infinitely increase the number of salt linkages. So the presence of the excess $-COO^-$ that cannot get involved in salt-linkage formation in AM48 or AM72 merely further promotes the absorption of water molecules in their bodies, resulting in their larger swelling ratios. The larger swelling ratio without the increase of the number of salt linkages merely lowers the molecular network density. Therefore the Young's moduli of AM48 and AM72 are smaller than those of AM1 and AM5.

4. Summary and conclusions

Amphoteric gel characteristics of swelling ratio, potential, and hardness were quantitatively evaluated and these characteristics were found to be under greater influence by –COOH groups than by $-NH_2$. These results are regarded as strong supportive evidence that the participation of $-COO^-$ created through the dissociation of –COOH in the formation of salt linkages has a predominant role in the hardness variation of amphoteric gels. Additionally, we speculated that the hydrogen bonds between –COOHs could also reinforce the anionic gel matrix to a large extent.

Acknowledgments

This research was conducted under the financial support of Health and Labor Science Research Grants of Research on Advanced Medical Technology (No. H14-nano-021) from the Ministry of Health Labor and Welfare and the Mikiya Science and Technology Foundation, both in Japan.

References

[1] T. Tanaka, Sci. Am. 244 (1981) 124.
[2] Y. Osada, S.B. Ross-Murphy, Sci. Am. 268 (1993) 82.
[3] H. Tamagawa, F. Nogata, S. Umemoto, N. Okui, S. Popovic, M. Taya, Bull. Chem. Soc. Jpn. 75 (2002) 383.
[4] H. Tamagawa, F. Nogata, T. Watanabe, A. Abe, J.-Y. Jin, S. Popovic, M. Taya, JSME Int. J. A 45 (2002) 579.
[5] A. Shozawa, Master's thesis, Tokyo Institute of Technology, 1987.
[6] I. Nakahara, Zairyourikigaku [Strength of Material], Yokendo, Tokyo, 1976 [in Japanese].
[7] T. Nakano, T. Tamagawa, T. Noagata, S. Ishihara, preprint, JSME Conference, 2001.
[8] G.N. Ling, In Search of the Physical Basis of Life, Plenum, New York/London, 1984.
[9] G.N. Ling, A Revolution in the Physiology of the Living Cell, Krieger, 1992.
[10] G.N. Ling, Life at the Cell and Below-Cell Level: The Hidden History of a Fundamental Revolution in Biology, Pacific Press, New York, 2001.
[11] G.N. Ling, Physiol. Chem. Phys. Med. NMR 29 (1997) 123.

Available online at www.sciencedirect.com
SCIENCE DIRECT
Journal of Membrane Science 243 (2004) 229–234
journal of MEMBRANE SCIENCE
www.elsevier.com/locate/memsci

Bending response of dehydrated ion exchange polymer membranes to the applied voltage

H. Tamagawa*, F. Nogata

Department of Human and Information Systems, Faculty of Engineering, Gifu University, 1-1 Yanagido, Gifu 501-1193, Japan

Received 15 March 2004; accepted 21 June 2004
Available online 26 August 2004

Abstract

Ion exchange polymer membrane in the dehydrated state was found to exhibit bending upon a small applied voltage, although the investigations on the hydrated ion exchange polymer membrane bending behavior have been performed quite intensively for more than a decade for the purpose of producing a practical polymer actuator. Our investigation on the dehydrated ion exchange polymer membrane has revealed that its bending direction is perfectly controllable by the polarity control of applied voltage and the degree of its bending curvature is also almost completely determined by the control of duration time of voltage application on it, while the hydrated ion exchange polymer membranes lack of such properties. Furthermore, the longevity of dehydrated ion exchange polymer membrane sustaining such a highly controllable properties has been found quite longer than that of the hydrated ion exchange polymer membrane.

Keywords: Selemion; Bending; Actuator; Hydrated; Dehydrated

1. Introduction

Producing a practical polymer actuator is a significant theme in the engineering field. For instance, one of ion exchange polymer membranes known as Nafion (Dupont) by the commercial name sandwiched between two thin metal layers exhibits a large bending upon a small applied voltage such as 1 V in the hydrated state, where Nafion contains the fixed anions and the free cations in the hydrated state [1–11]. Besides such a low consumption energy and a large deformation, its matrix is so soft and bending motion is quite supple, which must be quite beneficial for the purpose of making, for instance, a robot hand imitating a human hand motion. On the other hand, the conventional actuators such as a shape memory alloy and a piezoelectric, both of which consist of hard matrices, exhibit sometimes undesired too much straightforward motion. Therefore, polymer actuator will have a significant contribution to the industrial field and our actual life.

As described above, Nafion in the hydrated state exhibits a large bending upon a small applied voltage. It is a quite promising phenomenon, which could lead to the realization of a practical bending mode Nafion actuator. However, there are some problematic issues long hobbling the progress of this kind of polymer actuator researches. Such problems are listed as follows: (i) uncontrollability of the Nafion bending direction by the polarity control of applied voltage after its short use; (ii) large deviation of Nafion bending curvature from the desired curvature after its short use; (iii) the occurrence of bending relaxation; (iv) the short longevity.

One of the ion exchange membranes called Selemion (Asahi Glass Co., Ltd., Japan) sandwiched between two thin metal layers like Nafion, which contains the fixed anions and free cations in the hydrated state, also exhibits the bending upon an applied voltage. But it also has the same problematic issues as Nafion has – (i)–(iv) – in case we use it as a bending mode actuator material. Namely, regardless of ion exchange

* Corresponding author. Tel.: +81 58 293 2492/230 1111.
E-mail address: tmgwhrhs@cc.gifu-u.ac.jp (H. Tamagawa).

0376-7388/$ – see front matter © 2004 Elsevier B.V. All rights reserved.
doi:10.1016/j.memsci.2004.06.024

polymer membranes type, their bending mechanism must be the same and inevitably the same problems are accompanied for the realization of polymer actuator. Recently, the authors of this paper and our collaborator observed the relatively effective bending of dehydrated Selemion. Although it has been widely believed that the hydration has a requisite role for the induction bending of ion exchange polymer membrane under the applied voltage, it turned out, in fact, to be absolutely possible to induce the bending of dehydrated Selemion. Although the degree of its bending curvature is smaller than the hydrated one, still it is a visibly large enough. Our detailed investigation has revealed that the dehydration treatment on Selemion well overcomes the problematic issues (i)–(iv) described earlier, and it must be true for the other type of ion exchange polymer membranes. We report the detail on it in this paper.

2. Bending of ion exchange polymer membranes

First of all, the widely accepted bending mechanism of hydrated ion exchange membrane is explained.

2.1. Structure of a deformable ion exchange polymer membrane

As an example, we take up Na□on. Na□on is a sheet type polymer with the thickness of around 180 μm. Fig. 1 shows the molecular structure of Na□on. A large number of $-SO_3H$ groups are attached to the randomly folding □uorocarbon chains. Fig. 2 shows the Na□on sandwiched between two thin metal layers and it contains a large number of $-SO_3H$ functional groups. Both surfaces are metal plated and its matrix is hydrated.

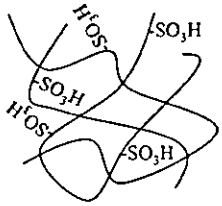

Fig. 1. Molecular structure of Na□on Main chains consist of □uorocarbon chain and $-SO_3H$ functional atomic groups are □xed as branches.

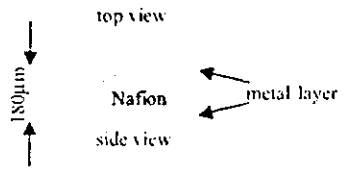

Fig. 2. The structure of Na□on sandwiched between two thin metal layers.

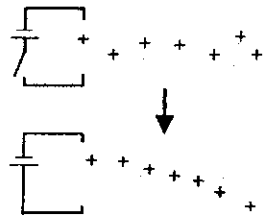

Fig. 3. Bending mechanism of Na□on. The shift of hydrated mobile cations toward the top surface direction by the applied electric □eld results in the gradient of swelling ratio of Na□on along its thickness direction, and it causes the downward bending of Na□on.

2.2. Bending mechanism

Application of voltage to Na□on causes its bending. It has been widely believed that the hydrated mobile cations contained in Na□on are dragged toward the top surface side of Na□on by the applied voltage – the top surface of Na□on is connected to the negative terminal of power supply – as depicted in Fig. 3, and it causes the gradient of swelling ratio of Na□on in its thickness direction, then consequently, the bending is induced (see Fig. 3 again). It could be speculated that this bending mechanism is not only true for Na□on bending but also true for other type of ion exchange polymer membranes bending as long as they contain the mobile ions in their hydrated state. For example, one of ion exchange membranes called Selemion in the hydrated state can be bent upon an applied voltage [7], where there are two type of Selemions that one is a cation exchange polymer membrane and the other one is an anion exchange polymer membrane, and we have con□rmed the induction of both of their bending.

3. Experimental

3.1. Materials

Selemion was employed as a starting material of a specimen. There are two types of Selemion as described above. We took up a Selemion of cation exchange type. The functional atomic group contained in this Selemion is $-SO_3H$ and it dissociates into $-SO_3^-$ and H^+ in the hydrated state. For the purpose of comparing the properties of Selemion with those of Na□on which has been long studied in order to produce a bending mode polymer actuator, Na□on was also employed for this study. Na□on contains $-SO_3H$ functional atomic groups, and they dissociate into $-SO_3^-$ and H^+ in the hydrated state.

3.2. Specimen preparation

Surfaces of Selemion were roughened with a sandpaper. They were plated with silver through the silver mirror reaction [8–10]. They were cut into strips with the dimension

of 20 mm-length × 2 mm-width. Some of them were stored in a 1 M HCl solution. This process imports the free ions, H^+ and Cl^-, into the Selemion body, and hereafter called hydrated–Selemion (H–S). The rest of them was stored in the desiccator for weeks so as to fully dehydrate, and hereafter called dehydrated–Selemion (D–S).

Na□on was also treated in the same way and cut into the same size of strips, and some of them stored in a 1 M HCl solution was designated as hydrated–Na□on (H–N), and the rest of them dehydrated and stored in the dessicator was designated dehydrated–Na□on (D–N).

3.3. Bending and controllability testing

Bending testing on all four types of specimens, H–S, D–S, H–N and D–S, was performed. Constant voltage was imposed on them, and their tip displacement was measured with a laser displacement meter as a function of time. From the tip displacement data, the specimen curvature was calculated as a function of time. Controllability of bending direction and curvature of these specimens are quite important factors for the purpose of producing polymer actuators. Therefore, we studied these factors through the investigation on the correlation between the bending direction and curvature of specimens and the polarity of applied voltage.

3.4. Oscillation testing

As described above, we had performed the bending testing on all four specimens already, yet it was performed under the condition of constant applied voltage. For the actuator use of ion exchange polymer membrane, it should behave (bend) in perfect agreement with the applied voltage that changes its voltage and polarity for long while. Therefore, oscillation testing was performed on all four types of specimens. Their bending curvature was measured as a function of time upon a sine curve type applied voltage.

4. Results and discussion

4.1. Bending and controllability testing

Fig. 4 shows the time dependence of H–N and H–S upon a constant applied voltage, 1 and 3 V. In this measurement, a strip of specimen with the size of 20 mm-length × 2 mm-width was □xed horizontally and connected to the power supply as depicted in Fig. 3. The bending curvature of specimen in a downward bending state is de□ned as a positive curvature, while that of in the upward bending state is de□ned as a negative curvature. At the initial stage, the higher applied voltage, 3 V, causes the larger bending for both specimens, but such a large bending curvature eventually relaxes with time. The bending relaxation must be caused by the □ow of water molecules contained in the specimen toward its bottom surface side. The lower applied voltage, 1 V, appears to sustain a fairly constant curvature of them. Here, we add some

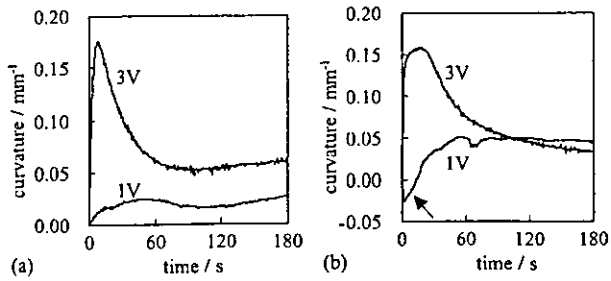

Fig. 4. Time dependence of bending curvature of (a) H–N and (b) H–S upon constant applied voltage, 1 and 3 V.

comment on the bending curvature behavior of H–S upon 1 V applied voltage. Right after the impose of 1 V on H–S, it exhibits upward bending as indicated by an arrow in Fig. 4(b). Although we have yet to identify the cause of it, we strongly speculate that the shift of hydrated anion (primarily hydrated Cl^- in this case) toward the bottom side of H–S induced the upward bending at the initial stage of bending – the bottom surface of H–S is connected to the positive terminal of power supply – as long as the conventionally accepted concept on the cause of bending described in Section 2.2 is right.

Next, we imposed the constant applied voltage on H–N and H–S but changed the voltage polarity periodically. Fig. 5 shows the results. At the moment indicated by arrows, the polarity change was given, where the absolute value of applied voltage had not been changed. None of specimens bending direction were well controlled by the polarity change. None of their bending curvatures were well controlled, either, and all of their curvature values decayed with time. Especially in case the applied voltage is 3 V, neither H–N nor H–S could recover their curvature to the positive side from the negative side after only □rst polarity change. It must be caused by the destruction of their matrices by the electrolysis of water contained in them. A 3 V applied voltage is so high enough to inevitably cause the vehement electrolysis of water.

Now the same measurements described so far is performed on D–N and D–S (no polarity change). D–N did not exhibit bending upon 1 nor 3 V constant applied voltage. D–S did not exhibit bending upon 1 V constant applied voltage (no

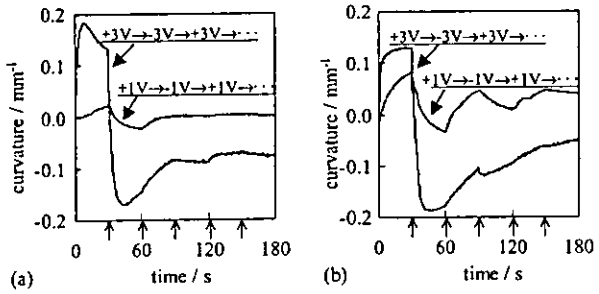

Fig. 5. Time dependence of bending curvature of (a) H–N and (b) H–S upon applied voltage with polarity change but whose absolute values are maintained at 1 and 3 V, namely, +1 V → −1 V → +1 V → ··· and +3 V → −3 V → +3 V → ···. Polarity change of applied voltage is given at the moments indicated by the arrows on the *x*-axis.

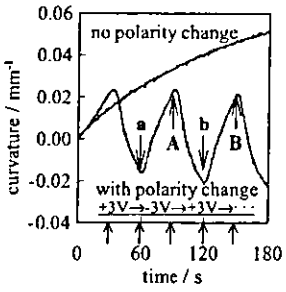

Fig. 6. Time dependence of bending curvature of D–S upon the constant (no polarity change) 3 V applied voltage and upon the 3 V applied voltage with polarity change but whose absolute value is maintained at 3 V where the polarity change is given at the moments indicated by the arrows on the x-axis.

polarity change), either, but it exhibited at 3 V constant applied voltage (no polarity change) as in Fig. 6. Although its curvature is smaller than the hydrated specimen H–S, no bending relaxation was accompanied. It is quite preferable for the actuator. Furthermore, D–S bending curvature perfectly follows the polarity change and the curvature value does not decay with time at all as also shown in Fig. 6. Furthermore, the value of bending curvature of D–S is well controlled by the duration time of applied voltage. For instance, the curvature indicated by the arrow-A in Fig. 6 is realized 30 s after the polarity change indicated by the arrow-a, and the bending curvature indicated by the arrow-B which is the same as that indicated by the arrow-A is also realized 30 s after the polarity change indicated by the arrow-b.

The similar excellent performance was in fact observed about D–N in case the higher voltage of 5 V was applied. But as intuitively understood, the lower consumption energy is better for its practical use. Therefore, we did not perform the further investigation on D–N, but only the observed time dependence of D–N bending curvature upon 5 V constant applied voltage is shown in Fig. 7. The bending is actually observed and no bending relaxation is observed unlike the hydrated Na□on, H–N. The reason of the higher voltage requirement for the D–N bending induction must lie in the thicker matrix of D–N than D–S. The thicker the specimen thickness, d, becomes, the lower the applied electric □eld, E, becomes, because E is given by $E = V/d$, where V is an applied voltage. The lower E hardly induces the thicker ion exchange polymer membrane bending.

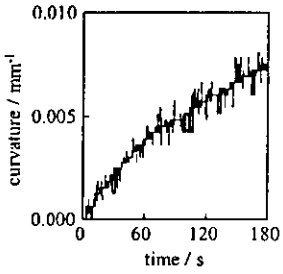

Fig. 7. Time dependence of bending curvature of D–N upon a constant applied voltage, 5 V.

Judging from the widely accepted bending mechanism described earlier, the creation of mobile hydrated ions through the hydration of ion exchange polymer membrane is requisite for the induction of bending. However, our research results suggest that the hydration is not in need for the induction of bending and no hydration bring us even better bending performance of ion exchange polymer membrane. No hydration eliminates the bending relaxation and the poor controllability of bending.

Now it is necessary to elucidate what causes the bending of D–S. Through the observation of D–S bending, we observed the color change of D–S surfaces. Always the surface connected to the negative terminal of power supply becomes white color, while the other surface connected to the positive terminal loses white color, and even through the repetitive polarity change, the surface connected to the negative terminal becomes always white and the other surface connected to the positive terminal always loses its white color accordingly. We measured the surface electric conductivity of D–S and found the high electric conductivity of the white colored surface and the fading of electric conductivity of the non-white colored surface. So this observation suggests that the white color originates from the color of silver, and the shift of silver layer from one surface to the other surface actually occurs in accordance with the change of polarity of power supply. We can strongly speculate that the shift of silver layer plays a critical role for the induction of D–S bending, but we have yet to □nd out the exact mechanism how it causes the bending. Someone may raise a question that a minute quantity of water remaining in D–S must contribute the creation of hydrated mobile ions in D–S and consequently results in its bending. However, we did not observe any gas bubbles generation from D–S body under 3 V of the applied voltage, when D–S is submerged in a silicone oil, where 3 V is high enough to cause the electrolysis of water generating H_2 and O_2 gases. Further, we did the following experiment. D–S used for a long while under 3 V loses its bending ability. Although we have not identi□ed the cause of bending ability loss, actually D–S loses its bending ability after long use. Since D–S was always used under 3 V for long while, we speculated that no water molecules remained in D–S body because of the water electrolysis. Dotite (Fujikura Kasei Co., Ltd., Tokyo) which is a mixture of silver powder and an adhesive polymer was spread on this long used D–S surfaces, then its bending ability was resurrected. Dotite does not contain any water molecules, therefore the bending of D–S is not caused by the existence of minute quantity of water molecules in it. Namely, the supplied silver on D–S surfaces from Dotite must have played some critical role for the induction of D–S bending. Therefore, silver has some essential role for the induction of bending.

4.2. Oscillation testing

Actuators should have a long and precise controllability for their practical use. In order to see if D–S has such a performance, the alternate voltage of sine curve, whose voltage

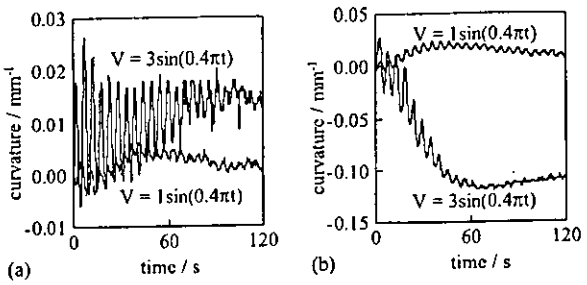

Fig. 8. Time dependence of bending curvature of (a) H–N and (b) H–S upon the alternate applied voltages, V (V) = 1 sin(0.4πt) and 3 sin(0.4πt), where t is the time.

is, namely, always changing, was imposed on it, and the time dependence of its curvature was measured. For comparison, the same measurements were performed about H–N and H–S, too. Fig. 8 shows the time dependence of H–N and H–S curvatures upon the alternate applied voltages V (V) = 1 sin(0.4πt) and 3 sin(0.4πt), where t is the time. All of them exhibit the oscillation of bending curvature in accordance with the frequency of applied voltage, 0.2 Hz. However, none of them sustains the same amplitude of bending curvature, actually they decay with time, while the amplitudes of applied voltages are maintained constant through the course of this experiment. And none of the center of oscillation of bending curvature is maintained constant at 0 mm^{-1}. They always largely deviate from 0 mm^{-1}, although the center of alternate applied voltage is maintained at 0 mV. On the other hand, the bending curvature amplitude of D–S upon the applied voltage, V (V) = 3 sin(0.4πt), is maintained almost constant, and the center of oscillation of bending curvature is maintained constant at 0 mm^{-1} as shown in Fig. 9. Someone may say that the bending curvature of D–S is so small compared with those of H–N and H–S in Fig. 8 and the center of oscillation of H–N and H–S bending curvature upon V (V) = 1 sin(0.4πt) is fairly close to 0 mm^{-1}. However, the bending curvature of D–S is still large enough so that we can detect it with our naked eyes and the bending curvature of H–N and H–S eventually diminishes toward 0 mm^{-1} after a while unlike that of D–S, and the deviation of the center of oscillation of bending curvature of H–N and H–S is quite large compared with that of D–S which is almost 0 mm^{-1} at any time. The regular oscillation of D–S bending curvature is sustained even at t = 600 s (the result is not shown, since it is hard to see the detail of bending curvature oscillation from the look of small size diagram). We add that it is true for the dehydrated Na□on, too, although a relatively high applied voltage is in need compared with D–S case. Therefore, besides such excellent bending properties of dehydrated ion exchange polymer membranes, they can acquire quite long longevity of bending performance through the dehydration treatment. If the bending is primarily cause by the shift of hydrated mobile ions, such an excellent and long sustainable bending behavior cannot be realized, since water molecules are easily decomposed into H_2 and O_2 through the electrolysis. Dehydration can let the ion exchange membranes exhibit the better performance, when they are used as the bending mode actuator materials.

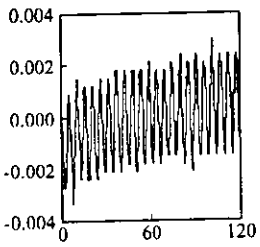

Fig. 9. Time dependence of bending curvature of D–S upon the alternate applied voltage, V (V) = 3 sin(0.4πt).

5. Conclusion

Dehydration of Selemion was found to be an e□cient method resulting in the precisely controllable bending of it with a longer longevity. The same was true for Na□on, too, and it let us speculate that any dehydrated ion exchange polymer membranes can be bent precisely at our will for a long period. Dehydration could become a new principle to realize a practical ion exchange polymer membrane actuator.

Acknowledgments

We would like to express our gratitude to Nihon Polymer (Aichi, Japan) and Asahi Glass Co., Ltd. (Tokyo, Japan) for their kind service to purchase Na□on and Selemion. This research was □nancially supported by Health and Labour Science Research Grants of Research on Advanced Medical Technology (No. H14-nano-021) from Ministry of Health Labour and Welfare, The Mikiya Science and Technology Foundation, and Izumi Science and Technology Foundation, all Japan.

References

[1] K. Oguro, Y. Kawami, H. Takenaka, Bending of an ion-conducting polymer □lm-electrode composite by an electric stimulus at low voltage, Trans. J. Micromach. Soc. 5 (1992) 27.
[2] K. Asaka, K. Oguro, Y. Nishimura, M. Mizuhara, H. Takenaka, Bending of polyelectrolyte membrane–platinum composites by electric stimuli I, response chracteristics to various waveforms, Polym. J. 27 (1995) 436.
[3] K. Salehpoor, M. Shahinpoor, M. Mojarrad, Actuators made from ion-exchange membrane–metal composites, smart materials technologies, Proc. SPIE Smart Mater. Struct. San Diego 3040 (1997) 192.
[4] M. Shahinpoor, M. Mojarrad, K. Salehpoor, Electrically induced large amplitude vibration and resonance characteristics of ionic polymeric membrane–metal composites arti□cial muscles, Proc. SPIE Smart Mater. Struct. San Diego 3041 (1997) 829.
[5] Y. Bar-Cohen, T. Xue, M. Shahinpoor, K. Salehpoor, J. Simpson, J. Smith, Low-mass muscle actuators using electroactive polymers (EAP), Proc. SPIE Smart Mater. Struct. San Diego 3324 (1998) 218.

[6] M. Uchida, M. Taya, Solid polymer electrolyte actuator using electrode reaction, Polymer 42 (2001) 9281.
[7] T. Nakagawa, Y. Takase, A. Abe, T. Watanabe, H. Tamagawa, F. Nogata, The bending characteristics of IPMCs containing fixed negative or positive charges under an electric field, JSME Conference preprint, Nagoya, Japan, 2003, p. 67.
[8] H. Tamagawa, F. Nogata, T. Watanabe, A. Abe, K. Yagasaki, Bending curvature and generated force by Nafion actuator, IEEE ICIT'02, Bankok, 2002, p. 945.
[9] H. Tamagawa, F. Noagata, T. Watanabe, A. Abe, K. Yagasaki, J.-Y. Jin, Influence of metal plating treatment on the electric response of Nafion, J. Mater. Sci. 38 (2003) 1039.
[10] H. Tamagawa, K. Yagasaki, F. Nogata, Mechanical characteristics of ionic polymer–metal composite in the process of self-bending, J. Appl. Phys. 92 (2002) 7614.
[11] S. Popovic, Design of electro-active polymer gels as acuator materials, PhD Thesis, University of Washington, 2001.